

Investigation of the Aerodynamic Drag of Baseballs with Gyro Spin [†]

Bin Lyu, Jeff Kensrud * and Lloyd Smith

School of Mechanical and Materials Engineering, Washington State University, Pullman, DC 99164, USA; bin.lyu@wsu.edu (B.L.); lvsmith@wsu.edu (L.S.)

* Correspondence: jkensrud.ssl@wsu.edu; Tel.: +01-509-335-4784

[†] Presented at the 13th conference of the International Sports Engineering Association, Online, 22–26 June 2020.

Published: 15 June 2020

Abstract: The following considers drag measurements of baseballs with backspin (spin axis horizontal and normal to trajectory) and gyro spin (spin axis parallel to trajectory) orientations. Balls were propelled through still air in a laboratory setting at 36 m/s and spin ranging from 1250 rpm to 1750 rpm. Balls were projected with backspin and gyro spin in the two- and four-seam orientations. Speed and position sensors measured the speed and location of the balls at three locations from which the coefficient of drag and lift were found. Drag was observed to depend on spin rate, spin axis and seam orientation. The largest and smallest coefficient of drag was found with the gyro four-seam and two-seam spin orientation, respectively. Drag was observed to correlate with seam height with back spin, but not with gyro spin. Lift was observed for baseballs with back spin, but not with gyro spin.

Keywords: gyro spin; backspin; drag; lift; seam height; baseball

1. Introduction

Drag, F_D , is the force acting in the direction opposing the ball's trajectory. Lift, F_L , is the force acting perpendicular to the ball's trajectory [1]. The drag and lift coefficients, C_D and C_L , are defined by

$$C_D = \frac{2F_D}{\rho AV^2}, C_L = \frac{2F_L}{\rho AV^2} \quad (1)$$

where ρ is the density of air, A is the cross-sectional area of the ball and V is the speed of the ball [1]. The cause of the drag force on the ball is related to flow separation from its surface. The drag on a baseball is important to understand when describing long trajectories, such as home runs. Small changes in drag result in large differences in carry distances [2]. For baseballs, the seams are large, and influence drag and airflow around the ball. Previous studies have found that the drag coefficient of a baseball is not constant, but depends on the seam orientation [3].

A baseball has two primary components of spin: transverse spin (known as back spin or top spin) and parallel spin (known as gyro spin) [4]. In this study, two spin axes, back and gyro, and two seam orientations, two-seam and four-seam, were compared (as shown in Figure 1).

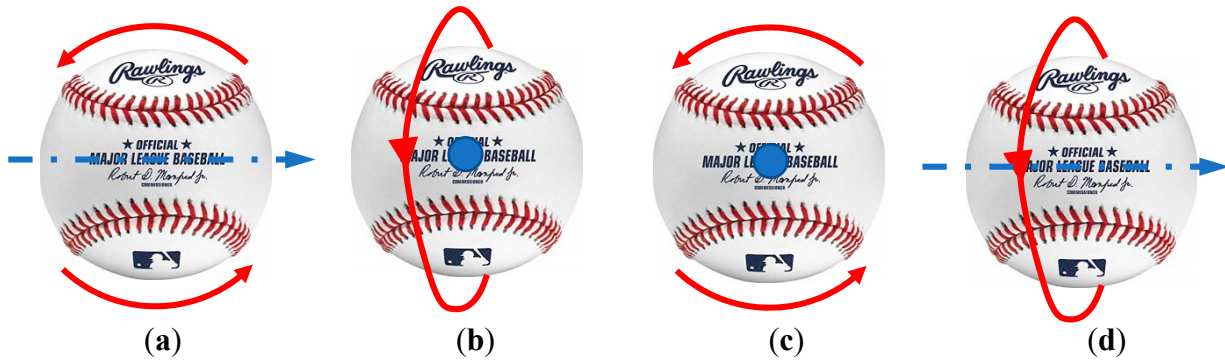


Figure 1. The direction of ball’s linear speed (blue arrow; a dot indicates that the ball goes into the page) and the direction of the spin (red arrow) for each orientation of the spin. (a) Four-seam back spin. (b) Two-seam back spin. (c) Four-seam gyro spin. (d) Two-seam gyro spin.

Due to the difficulties of projecting baseballs with gyro spin, few studies have measured the drag and lift coefficient from this spin axis. Yokoyama measured the drag coefficient of gyro spinning baseballs by recording the ball’s trajectory using high-speed cameras [5]. Himeno compared CFD (Computational fluid dynamics) to a trajectory tracking method to calculate the drag coefficient of a gyro spinning baseball, but did not find good agreement between the two methods [6]. Nagami used high speed video to track pitches and describe the relationship between lift and spin for different pitch types [7]. Previous aerodynamic studies have shown that the drag coefficient of a baseball is correlated with seam height [8]. However, the spin axis was not considered in this work, preventing evaluation of gyro spin.

The aim of this study was twofold: firstly, to measure the drag and lift coefficients of baseballs with different spin orientations in still air; secondly, to characterize the dependence of the seam orientation and spin axis of baseballs on the drag coefficient.

2. Method

This study considered nine MLB baseballs. Each ball was projected with four spin and seam orientations: four-seam back spin, two-seam back spin, four-seam gyro spin and two-seam gyro spin. The drag coefficient was found and compared between each orientation at the same speed and spin rate.

A bespoke, non-wheeled pitching machine was used to project the baseball at the target speed and spin rate without damaging the surface of the ball (shown in Figure 2). To impart back spin, a flexible tip [9] was coupled to a pneumatic linear accelerator. High and low friction materials were attached to opposite sides of the tip to generate torque about the center of the ball. Spin was controlled by changing the length and compressive force of the tip on the ball. A separate mechanical link was used to impart gyro spin which applied a torque parallel to the ball trajectory axis, using a tip with equal friction on both sides.



Figure 2. Setup of the pitch machine to project baseballs with desired spin rate and spin axis.

Ball speed and location were measured at three locations along the flight path, as shown in Figure 3. Sensors measured speed from successive pairs (0.41 m apart) of light gates (Ibeam, ADC). The distance, *d*, between the first and third speed sensors was 8.95 m, while the heights were within 0.025m of each other. Sensors were placed to maximize the distance between them, while minimizing the change in trajectory angle (the vertical component of velocity was 1.34 m/s or less) with respect

to the horizontal plane. The ball’s vertical location was measured at each speed sensor and used to calculate the lift force. A high speed video camera (Phantom V711 at 2000 fps) was used to record each shot to verify spin rate, spin axis, and seam orientation. The drag force was found from

$$F_D = m \frac{V_3^2 - V_1^2}{2d} \tag{2}$$

where V_1 and V_3 were the speeds at the first and third sensors, respectively, and m was the ball mass. The lift force was found from

$$F_L = m \left(\frac{2(D_y - V_y t_2)}{t_2^2} - g \right) \tag{3}$$

where D_y was the vertical change in ball position between the second and third speed sensors, V_y was the vertical velocity at the second speed sensor, t_2 was the time for the ball to travel from the second speed sensor to the third speed sensor, and g was gravitational acceleration. The vertical component of velocity at the second sensor, V_y , was calculated from the known speeds and locations at all three sensors. Details of the lift and drag measurements may be found elsewhere [10].

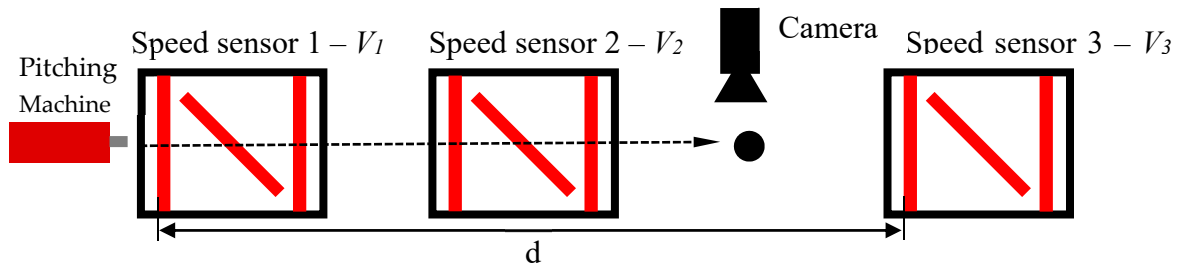


Figure 3. Arrangement of the pitching machine, speed sensors and camera to measure ball speed, rotation and location. The gate aligned vertically measured ball speed, while the angled gates measured position.

The surface profile of the baseballs was measured with a non-contact laser profiler (as shown in Figure 4). Seam height was taken from the difference of the ball peak radius at the seam and the radius of the panel adjacent to the seam. For each ball, seam height was taken from the average of 32 measurements.



Figure 4. Laser profiler used to measure seam height of baseballs.

3. Calibration and Uncertainty

The coefficient of lift and drag were calibrated daily, prior to testing. The speed and spin rate of the calibration shots were the same as those used for the test balls. To calibrate drag, a smooth sphere (diameter = 7.59 cm) and a dimpled ball (diameter = 7.18 cm) were projected through the system at the start of each test day. The drag measuring system was considered calibrated when the average C_D of three shots was within ± 0.01 of its known value. To calibrate lift, a setup baseball was projected with a vertical spin axis to eliminate the Magnus effect in the vertical direction. Lift was considered calibrated when the average C_L from three consecutive shots was 0.00 ± 0.01 .

The precision of the speed sensor was 0.025% of the measured speed. Accordingly, the uncertainty of C_D and C_L for a baseball were 0.003 and 0.0005, respectively. Other factors can affect the uncertainty of the drag and lift measurement, including the error from air properties and position measurement. Random error was analyzed by measuring the variance of 480 balls at 35.7 m/s. Each ball–speed combination consisted of four repeat shots. The average standard deviation of the drag and lift coefficient was 0.007 for a baseball traveling at 35.7 m/s with 2500 rpm.

4. Results

Each baseball was projected at a speed of 35.8 ± 0.9 m/s, and a spin rate at 1500 ± 250 rpm. The lift and drag coefficient of each orientation for each ball was calculated from the average of four repeat shots.

4.1. Drag

The average drag coefficient of all nine baseballs was measured to compare the difference between the spin orientations. As is shown in Figure 5, balls with a two-seam gyro spin showed the lowest average drag, with $C_D = 0.29$. Balls with a four-seam gyro spin showed the highest average drag, with $C_D = 0.37$. Balls with a four-seam and two-seam back spin had $C_D = 0.33$ and $C_D = 0.32$, respectively. These results indicate that the drag coefficient was sensitive to the ball orientation for gyro spin, but not for back spin.

4.2. Lift

The average lift coefficient of the nine baseballs was measured to compare the difference between the spin orientations. As is shown in Figure 5, the two-seam and four-seam gyro spin had negligible Magnus force, where the average lift in the gyro orientations were 0.01 and -0.01 , respectively. This was expected and agrees with other work [11]. The lift coefficient for the two-seam and four-seam back spin was 0.17 and 0.18, respectively. These results agreed with the lift coefficients from a previous study involving MLB (Major League Baseball) baseballs [12].

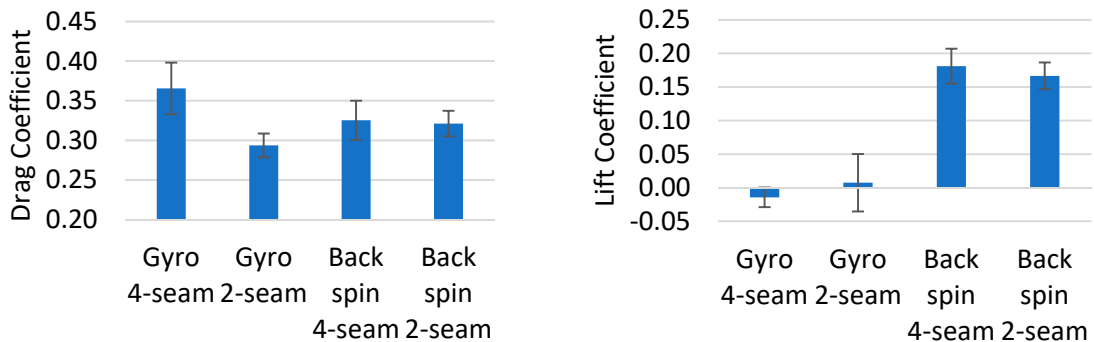


Figure 5. Average drag (left) and lift (right) coefficient of nine tested baseballs for each spin orientation. Each column indicates the average of nine baseballs.

4.3. Seam Height

A dependence was observed between the seam height and the drag coefficient of back spinning baseballs (Figure 6). The strongest correlation was observed for baseballs with a four-seam back spin, with $R^2 = 0.72$. For baseballs with a two-seam back spin, $R^2 = 0.51$. The drag on baseballs with gyro spin showed little correlation with seam height, where $R^2 < 0.1$.

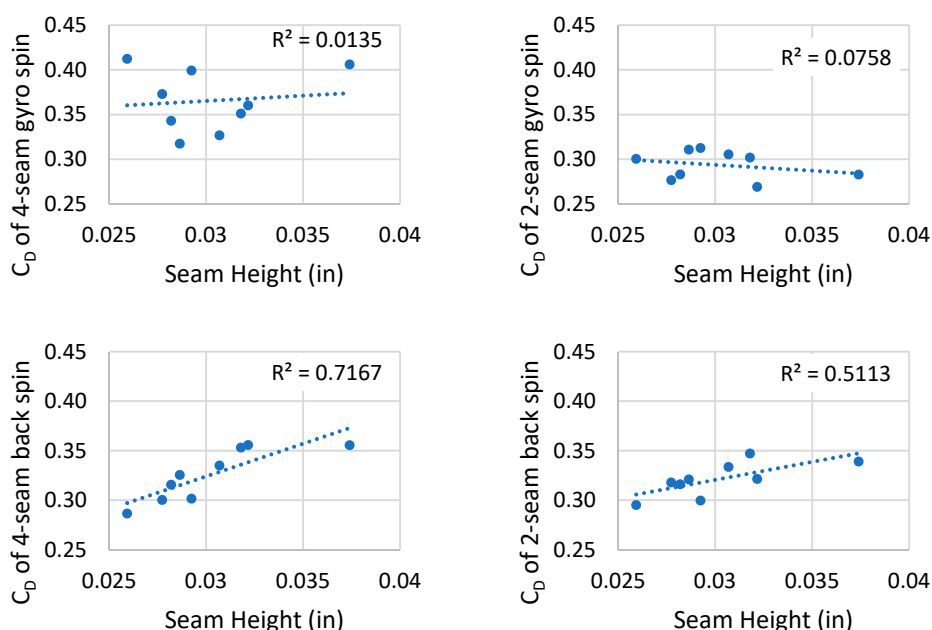


Figure 6. Drag coefficient of baseballs with different spin orientations as a function of seam height. Each data point indicates one baseball.

5. Discussion

A strong correlation between seam height and the drag coefficient was observed for back spin, but not for gyro spin. For back spin, a high seam will have a greater influence on the separation point (as it passes through the flow separation region) than a low seam, giving rise to a sensitivity of drag to seam height. For gyro spin, the seam is always in the separation region, so the separation point will be fixed for high and low seam balls, giving rise to a low sensitivity of drag to seam height.

The air flow velocity is highest near the ball surface furthest from the spinning axis; in the following, this will be referred to as the max flow air. The baseball will have a higher drag coefficient when more seams are exposed to the max flow air. A seam exposure index (S_e) can be defined from the amount of seam exposed to max flow air for each spin orientation as

$$S_e = dnt \tag{4}$$

where d is the length of each seam exposed to the max flow, n is the number of the seams and t is the ratio of time for which each seam is exposed for each spin revolution.

The seam exposure index for each orientation is listed in Table 1. For the four-seam back spin, as shown in Figure 7a, the length of the exposed seam is highlighted by red lines. Each seam is exposed twice (one on the top, one on the bottom) during each revolution. For the two-seam back spin, as shown in Figure 7b, the length of the exposed seam is the width of the seams. When the baseball is spinning in this orientation, about 75° of the max flow air region does not have a seam. When that region is on the top or bottom, $n = 2$. Otherwise, $n = 4$. For the four-seam and two-seam gyro spin, as shown in Figure 7c, d, the length of the exposed seam is the width of the seams.

Table 1. Calculation of S_e for Each Orientation.

	Orientation				
	a	b	c	d	
d	7.62	0.91	0.91	0.91	
n	4	2	4	2	
t	8.10%	41.67%	58.33%	100%	100%
S_e	2.47	2.88	3.64	1.82	

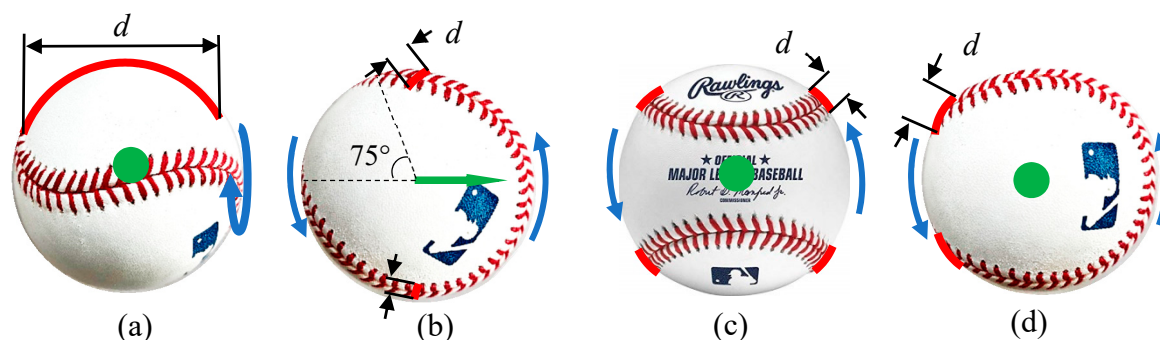


Figure 7. Seams exposed to the max flow for each spin orientation. The green dot or arrow indicates the speed direction, the blue arrow indicates rotation direction and the red line highlights the seams that are exposed to the max flow at that ball orientation. (a) Four-seam back spin. (b) Two-seam back spin. (c) Four-seam gyro spin. (d) Two-seam gyro spin.

Figure 8 compares the drag coefficient and seam exposure index for each orientation. A strong correlation was observed between S_e and the average drag coefficient for each spin orientation. The results show that the location of the seam in the airflow plays an important role in understanding its effects on drag.

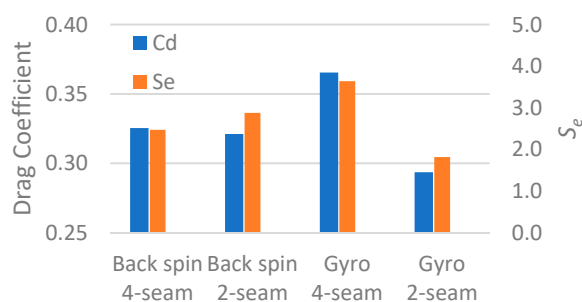


Figure 8. The comparison between S_e and the average drag coefficient of each spin orientation.

6. Conclusions

This study considered the lift and drag measurement of baseballs in four different spin orientations. The study found a strong correlation between seam height and the coefficient of drag for balls in the back spin orientation, where drag increased with seam height. A correlation between drag and seam height was not observed for the baseballs with gyro spin, suggesting seam height alone does not influence drag. A new parameter, S_e , was defined, which showed that, as more seams are exposed to the max flow air, the drag coefficient increases. The highest and lowest drag coefficients found here were in the four-seam and two-seam gyro spin orientations, respectively. The lift coefficient was also measured, and supported other findings where lift was the greatest in backspin and negligible for gyro spin.

Conflicts of Interest: The authors declare no conflict of interest.

Reference

1. Elger, D.F.; Roberson, J.A. *Engineering Fluid Mechanics*; Wiley: Hoboken, NJ, USA, 2013.
2. Albert, J.; Bartroff, J.; Blandford, R.; Brooks, D.; Derenski, J.; Goldstein, L.; Hosoi, A.P.; Lorden, G.; Nathan, A.; Smith, L. *Report of the Committee Studying Home Run Rates in Major League Baseball*; MLB, New York, NY, USA, 2018.
3. Himeno, R. Computational study of influences of a seam line of a ball for baseball on flows. *J. Vis.* **2001**, *4*, 197–207.

4. Nathan, A.M. *Determining the 3D Spin Axis from Statcast Data*; University of Illinois, Urbana, IL, USA 2018.
5. Yokoyama, Y.; Miyazaki, T.; Himeno, R. Drag crisis of gyro-balls. *J. Jpn. Soc. Fluid Mech. NAGARE* **2008**, *27*, 403–409.
6. Himeno, R.; Miyazaki, T. Aerodynamics of baseball. In Proceedings of the ISBS-Conference Proceedings Archive, Tsukuba, Japan, 18–22 July 2016.
7. Nagami, T.; Higuchi, T.; Nakata, H.; Yanai, T.; Kanosue, K. Relation between lift force and ball spin for different baseball pitches. *J. Appl. Biomech.* **2016**, *32*, 196–204.
8. Kensrud, J.R.; Smith, L.V.; Nathan, A.; Nevins, D. Relating baseball seam height to carry distance. *Procedia Eng.* **2015**, *112*, 406–411.
9. Kensrud, J. *Flex Grip Sports Ball Pitching Machine Tip*. PCT/US2017/032887, The International Bureau of WIPO, Geneva, Switzerland, 2018.
10. Kensrud, J.R. Determining Aerodynamic Properties of Sports Balls in Situ. Master's Thesis, Washington State University, Pullman, WA, USA, 2010.
11. Nathan, A.; Baldwin, D. An Analysis of the Gyroball. *Baseb. Res. J.* **2007**, *36*, 77–80.
12. Kensrud, J.R.; Smith, L.V. In situ lift measurement of sports balls. *Procedia Eng.* **2011**, *13*, 278–283.



© 2020 by the authors. Licensee MDPI, Basel, Switzerland. This article is an open access article distributed under the terms and conditions of the Creative Commons Attribution (CC BY) license (<http://creativecommons.org/licenses/by/4.0/>).